Journal of Information Display
Vol. 13, No. 1, March 2012, 7–16

Taylor & Francis
Taylor & Francis Group

Color accuracy of imaging using color filters

P. Boher, T. Leroux, V. Collomb Patton and T. Bignon

ELDIM, 1185 Rue d'Epron, F14200 Hérouville Saint Clair, France

In this paper, the problem concerning the color accuracy of imaging systems using color filters is examined. It is shown that the only solution to the problem is to build systems with the spectral response matching the CIE curves as closely as possible. If the spectral response does not closely match the CIE curves, it was demonstrated that calibration cannot solve the problem and will result in very unstable colorimeters. A practical solution that uses telecentric lenses on the sensor side in addition to dedicated color filters for each CCD detector is presented. For systems that closely match the CIE curves, an innovative method of improving the color accuracy based on the precise measurement of the spectral response is presented. The small discrepancies in the spectral response with regard to the CIE curves are corrected in different ways during the measurements. Finally, it is shown that the tristimulus calibration that is used for display measurement is very unstable for systems without CIE matching and is much more stable with systems that closely match the CIE curves.

Keywords: color; CIE curves; telecentric objective; tristimulus

1. Introduction

Accurate color assessment is essential in many applications. Based on the intrinsic differences in the mechanisms of the measurement devices, there are three types of colorimetry systems: spectroradiometers, spectrophotometers, and tristimulus colorimeters. The tristimulus filter-type colorimeters are the most widely used for imaging applications. Many studies have been conducted on how to calibrate tristimulus filter-type colorimeters, but the results are always strongly related to the calibration conditions and the target stimulus [1,2]. These authors are interested in a system that can make accurate color measurements for any type of stimulus.

Modern digital cameras have sensors for the red (R), green (G), and blue (B) primary colors, which are sensitive to a range of wavelengths for color acquisition. These sensors' sensitivity to each wavelength, however, is not identical to the sensitivity to the corresponding wavelength of the sensors in the human eye. Thus, the camera response is not colorimetric, and the resulting RGB values are not linear transforms of the device-independent tristimulus values based on the CIE-color-matching functions. In addition, the RGB signals generated by digital cameras are device-dependent, and a strong color difference can be observed for the same object measured by different cameras. This is why the problem of a device-independent digital *XYZ* camera has been examined by many researchers [3–8]. Linear combinations of CIE-color-matching functions have for instance been used to design three-filter cameras following the Luther condition [9]. Nevertheless, it is always difficult to adjust the spectral sensitivity due to the problems in the practical production of filters, sensors, and lenses, and the impact on the color error has not been thoroughly studied.

In the following, using the definition of color measurement, it is shown that if color accuracy is desired for any working condition, the only way to achieve it is to come up with a system that closely matches the CIE curves at any wavelength. In addition, the use of linear combinations of CIE-color-matching functions in some cases results in a drastic rise in the requirements of the resulting filters. In this paper, how to realize high-accuracy colorimeters using an optical design that presents a light collection efficiency that is independent of the object's distance is shown. The method of realizing dedicated color filters for each detection system is also presented. In addition, different methods of correcting the color measurements using the measured spectral deviation of the response of the system with regard to the CIE curves are presented. It is also demonstrated that the standard tristimulus calibration technique [9,10] is much more stable when used on a system closely matched to the CIE curves.

2. Theory

2.1. CIE curves

Colorimetric measurements are based on the measurement of the tristimulus values X, Y, and Z. These quantities must be measured according to the three normalized CIE spectral-response curves [(cf. Figure 1(a)] [11], as follows:

$$X = \int_{380}^{780} f(\lambda)\bar{x}(\lambda)\,\mathrm{d}\lambda,$$

*Corresponding author. Email : pboher@eldim.fr

ISSN 1598-0316 print/ISSN 2158-1606 online

http://dx.doi.org/10.1080/15980316.2012.652204
http://www.tandfonline.com

$$Y = \int_{380}^{780} f(\lambda)\bar{y}(\lambda)\,\mathrm{d}\lambda,$$
$$Z = \int_{380}^{780} f(\lambda)\bar{z}(\lambda)\,\mathrm{d}\lambda,$$

where $f(\lambda)$ is the spectral stimulus that will be measured herein, and $\bar{x}$, $\bar{y}$, and $\bar{z}$ are the three CIE-color-matching functions. The colorimetric coordinates are expressed by

$$x = \frac{X}{X+Y+Z},$$
$$y = \frac{Y}{X+Y+Z},$$
$$z = \frac{Z}{X+Y+Z}.$$

2.2. *Color accuracy and spectral matching*

As the X, Y, and Z values are the results of a convolution between the spectral stimulus and the spectral responses of each measurement channel of the equipment, the best accuracy must be maintained for these channels all over the spectrum. For a given color accuracy, a precise computation of the spectral-response accuracy requirements can be done. Indeed, by using a standard method of error propagation, the following equations can be formulated:

$$\mathrm{d}x = \left|\frac{\partial x}{\partial X}\right|\mathrm{d}X + \left|\frac{\partial x}{\partial Y}\right|\mathrm{d}Y + \left|\frac{\partial x}{\partial Z}\right|\mathrm{d}Z,$$
$$\mathrm{d}y = \left|\frac{\partial y}{\partial X}\right|\mathrm{d}X + \left|\frac{\partial y}{\partial Y}\right|\mathrm{d}Y + \left|\frac{\partial y}{\partial Z}\right|\mathrm{d}Z,$$
$$\mathrm{d}z = \left|\frac{\partial z}{\partial X}\right|\mathrm{d}X + \left|\frac{\partial z}{\partial Y}\right|\mathrm{d}Y + \left|\frac{\partial z}{\partial Z}\right|\mathrm{d}Z.$$

Using the expressions of the x, y, and z color coordinates, these authors find the following conditions where

$$\mathrm{d}x = (1-x)\frac{dX}{X+Y+Z} + x\frac{dY}{X+Y+Z} + x\frac{dZ}{X+Y+Z} < \varepsilon, \quad (1)$$
$$\mathrm{d}y = y\frac{dX}{X+Y+Z} + (1-y)\frac{dY}{X+Y+Z} + y\frac{dZ}{X+Y+Z} < \varepsilon, \quad (2)$$
$$\mathrm{d}z = z\frac{dX}{X+Y+Z} + z\frac{dY}{X+Y+Z} + (1-z)\frac{dZ}{X+Y+Z} < \varepsilon. \quad (3)$$

If the following equations can be verified, Equations (1)–(3) are also verified:

$$\frac{dX}{X} \le \frac{\varepsilon}{2x(1-x)}, \quad (4)$$
$$\frac{dY}{Y} \le \frac{\varepsilon}{2y(1-y)}, \quad (5)$$
$$\frac{dZ}{Z} \le \frac{\varepsilon}{2z(1-z)}. \quad (6)$$

Using Equations (4)–(6), the accuracy of the spectral-response matching on the CIE curves can be easily quantified for a given color error ε. As shown in Figure 1(b), to achieve a moderate color accuracy of 0.003, a maximum error of less than 1% is required on the spectral-response matching of the X, Y, and Z filters at all wavelengths when the CIE response function is higher than 10% of its maximum [cf. Figure 1(a) and (b)].

2.3. *Linear combinations of the CIE-color-matching functions*

A number of papers have presented a design of an XYZ camera using a single sensor and linear color-matching functions [3–8]. The idea is to adjust the spectral response of the system not directly on the XYZ CIE curves but on a linear combination of these functions. In practice, additional

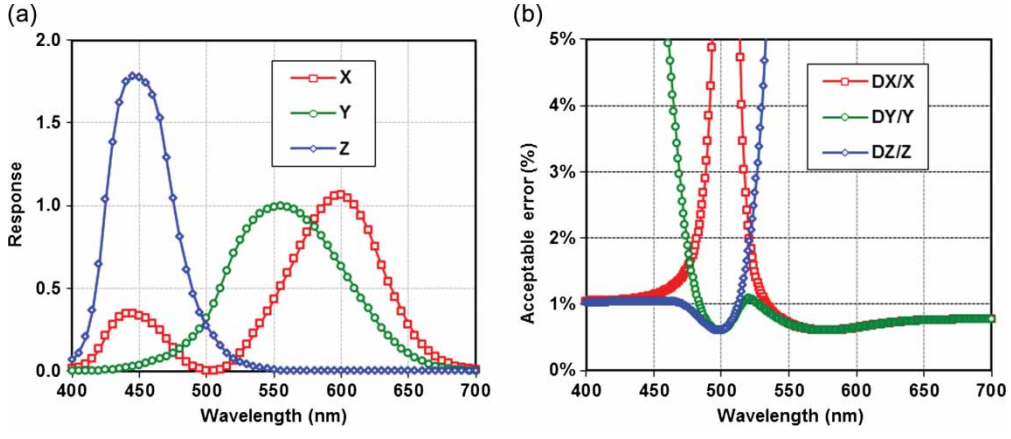

Figure 1. (a) $\bar{x}$, $\bar{y}$, and $\bar{z}$ CIE curves (CIE 2° 1931). (b) Acceptable spectral-response-matching error of the CIE curves for an overall color error of 0.003.

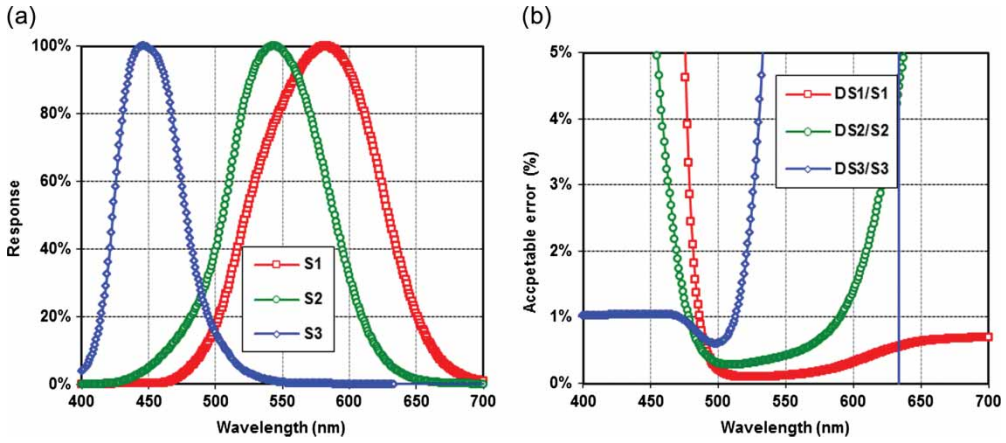

Figure 2. (a) S_i curves and (b) acceptable spectral-response-matching error of the CIE curves for an overall color error of 0.003.

conditions are introduced, such as the positivity of the functions, a single peak by function, and a small overlap between them. A set of a_{ij} coefficients is deduced, as follows [3,4]:

$$\begin{pmatrix} X \\ Y \\ Z \end{pmatrix} = \begin{pmatrix} a_{11} & a_{12} & a_{13} \\ a_{21} & a_{22} & a_{23} \\ a_{31} & a_{32} & a_{33} \end{pmatrix} \begin{pmatrix} S_1 \\ S_2 \\ S_3 \end{pmatrix}.$$

It is interesting to examine the requirements in terms of curve matching for this type of solution. Calculating the sum of Equations (1)–(3) will yield the following:

$$\mathrm{d}x + \mathrm{d}y + \mathrm{d}z = 2(1-x)\frac{dX}{X+Y+Z} + 2(1-y)\frac{dY}{X+Y+Z} + 2(1-z)\frac{dZ}{X+Y+Z} < 3\varepsilon.$$

If the variables in the S_i space will be converted, the following can be easily obtained:

$$[(1-x)a_{11} + (1-y)a_{21} + (1-z)a_{31}]\,\mathrm{d}S_1 + [(1-x)a_{12} + (1-y)a_{22} + (1-z)a_{32}]\,\mathrm{d}S_2 + [(1-x)a_{13} + (1-y)a_{23} + (1-z)a_{33}]\,\mathrm{d}S_3 < \frac{3\varepsilon}{2}(X+Y+Z).$$

One sufficient condition can be written as follows

$$\frac{dS_1}{S_1} < \varepsilon \frac{X+Y+Z}{(2S_1[(1-x)a_{11} + (1-y)a_{21} + (1-z)a_{31}])} \quad (7)$$

$$\frac{dS_2}{S_2} < \varepsilon \frac{X+Y+Z}{(2S_2[(1-x)a_{12} + (1-y)a_{22} + (1-z)a_{32}])} \quad (8)$$

$$\frac{dS_3}{S_3} < \varepsilon \frac{X+Y+Z}{(2S_3[(1-x)a_{13} + (1-y)a_{23} + (1-z)a_{33}])}. \quad (9)$$

Using Equations (7)–(9), the accuracy of the spectral-response matching can be easily quantified on the S_i curves for a given color error ε. The set of coefficients proposed in reference [7] is as follows:

$$\begin{pmatrix} X \\ Y \\ Z \end{pmatrix} = \begin{pmatrix} 1.3994 & -0.7355 & 0.3716 \\ 0.4662 & 0.6169 & 0.0079 \\ 0.0001 & -0.0002 & 1.7834 \end{pmatrix}^{-1} \begin{pmatrix} S_1 \\ S_2 \\ S_3 \end{pmatrix}.$$

The corresponding S_i functions are shown in Figure 2(a), and the acceptable errors calculated using Equations (7)–(9) for a color error of 0.003 are shown in Figure 2(b). If the S_i functions seem quite attractive particularly because of the occurrence of only one peak for the S_1 curve, the acceptable errors that are needed with these new functions are substantially decreased. This is particularly true for the S_1 curve at around 500 nm, where the X curve approaches zero [cf. Figure 1(a)]. In this wavelength range, the acceptable error for the S_1 curve is below 0.1%, a value that is definitely impracticable. The conclusion is that a colorimeter with high accuracy under all working conditions can be made only by coming up with a system with a spectral response matching the CIE curves as closely as possible.

3. Experimental system

3.1. Optical design of the color filter system

The imaging videocolorimeter is based on a Peltier-cooled CCD sensor with a true 16-bit analog digital converter. Different imaging objectives are available (with an 8°, 16°, or 30° maximum angular aperture). Each objective is telecentric on the sensor side to ensure the same transmittance of the filters in the entire field of view of the system, which is fundamental for spectral-response matching, and consequently, for color accuracy (cf. Section 2). In addition, this configuration ensures that the collection efficiency is independent of the distance to object L. This important property can be easily demonstrated by calculating the flux emitted by elemental surface $\mathrm{d}S_2$ of luminance L in small angular-cone $2\theta_2$ for both configurations (cf. Figure 3).

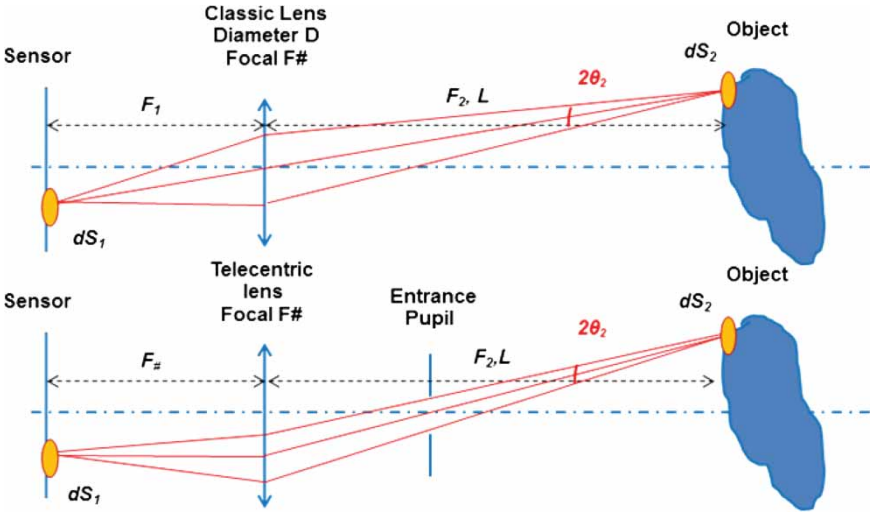

Figure 3. Standard imaging objective (top) and imaging objective with a telecentric lens on the sensor side (bottom).

The standard imaging is given by [12,13]

$$\mathrm{d}\Phi_2 = 2\pi L(1-\cos\theta_2)\,\mathrm{d}S_2 \approx \pi L\theta_2^2\,\mathrm{d}S_2.$$

The flux collected by and elemental surface dS_1 on the detector is given by

$$\mathrm{d}\Phi_1 = k\mathrm{d}\Phi_2 = k\pi L\theta_2^2\mathrm{d}S_2 = M_1\,\mathrm{d}S_1.$$

where k is the transmittance of the objective. The conservation of the geometric etendue to produce the following relation between the emission and the collection surfaces:

$$\frac{dS_1}{F_1^2} = \frac{dS_2}{F_2^2}.$$

where F_1 and F_2 are the focal distances for the detection and emission sides, respectively (cf. Figure 3). If D is the diameter of the objective, angle θ_2 can be obtained using the following equation:

$$\theta_2 = \tan^{-1}(D/2F2) \approx \frac{D}{2F_2}.$$

Using the relation between F_1, F_2, and focal length $F\#$, as shown in the following equation:

$$\frac{1}{F\#} = \frac{1}{F_1} + \frac{1}{F_2}.$$

the following can finally be obtained:

$$M_1 = \frac{k\pi LD^2}{4F\#^2}\left(1-\frac{2F\#}{F_2}\right) = M_\infty\left(1-\frac{2F\#}{F_2}\right). \quad (10)$$

The signal seen by the detector is thus dependent on the distance of the object. At $10F\#$, the reduction is about 20%, as shown in Figure 4, with a big impact on accuracy. This means that a videocolorimeter using the standard imaging optics needs to be calibrated for the different distances of the object under investigation.

For a telecentric configuration

$$\frac{dS_1}{F\#^2} = \frac{dS}{L^2}.$$

M_1 is independent of the distance in the first approximation. If the cosines will be developed to the third term, it will be found that

$$M_1 = \frac{k\pi LD^2}{4F\#^2}\left(1-\frac{3F\#^2}{16F_2^2}\right) = M_\infty\left(1-\frac{3F\#^2}{16F_2^2}\right). \quad (11)$$

Figure 4 shows a flux reduction lower than 1% for $5F\#$ distance, and lower than 0.1% for $15F\#$. A single calibration is then sufficient for all practical distances, a characteristic that is fundamental for the simplicity of the use of such instrument as well as for color accuracy.

3.2. *Absolute spectral response*

For each optical system, the spectral response is measured with regard to an NIST reference photodiode [14]. The light emitted by a stabilized xenon source goes across a monochromator and is injected into an optical system with a beam splitter. Part of the light is measured by the optical system or the NIST reference photodiode, and by another parallel photodiode. The wavelength scan within the visible range is realized two times: one with the optical system to be calibrated, and one with the reference photodiode. The relative spectral response is deduced (cf. Figure 5). As shown in Figure 5, each system has a different spectral response even if the shape of the curve is the same for the same CCD types. This is due to the small variations both in the fabrication process of the sensor and of the optics. Even if they are small, these variations must be taken into account so that the color filter design will match the CIE curves as closely as possible.

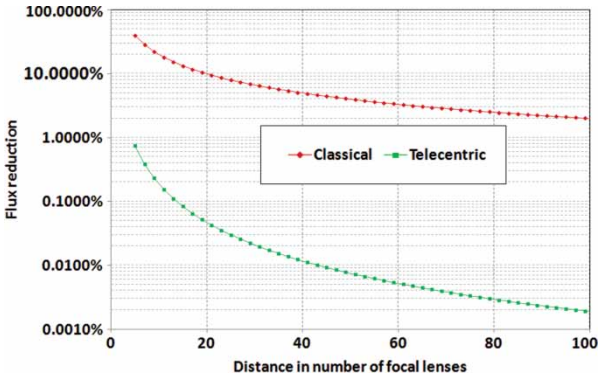

Figure 4. Collection efficiency of the standard imaging objective and the telecentric imaging objective on the sensor side.

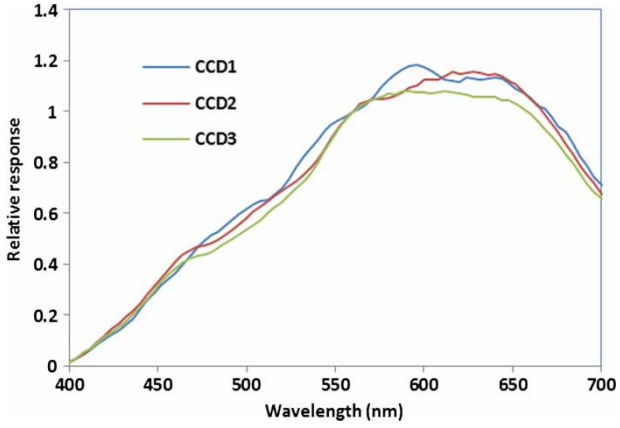

Figure 5. Relative spectral response of three different videocolorimeters.

3.3. *Design of the color filters*

The color filters are realized using different color glasses. For a given filter, the thicknesses of the different glasses are adjusted to obtain transmittance values that match each CIE curve with maximum accuracy when combined with the CCD spectral response. For the *Z* CIE curve, one filter is used. One example of a filter structure is shown in Figure 6, with the resulting transmittance. The *X* curve is generally matched with a combination of two filters, one for the peak in the blue color and one for the peak in the red color. The luminance CIE curve is also matched with two filters due to the large bandwidth of the *Y* CIE curve. A set of five color filters is shown in Figure 6 as an example. The best resulting CIE matching is shown in Figure 7(a). It can be seen that the adjustment is not very good in this case. This system was selected to illustrate the technique of more easily increasing the color accuracy (cf. Section 4). Better color matching can be obtained with the same technique on other systems, as also shown in Figure 7(b).

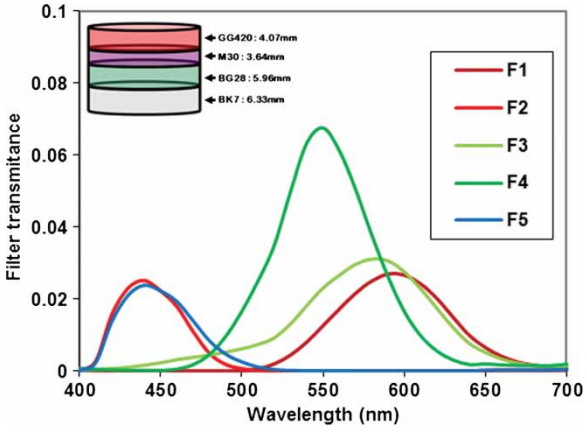

Figure 6. Transmittance of the five color filters of one videocolorimeter. The structure of the *Z* filter (F5 filter) is also shown.

4. Methods of increasing the color accuracy

4.1. *With knowledge of the spectral stimulus*

Using the measured spectral response for each color filter makes it easy to compute the best coefficients that give a perfect match of the CIE curves for each monochromatic stimulus. Such coefficients are shown in Figure 8 for the system of the spectral response shown in Figure 7(a). For the *Z* CIE curve, the inversion is straightforward because there is only one filter. For the two other CIE curves, coefficients that are as flat as possible were selected. As can be seen in Figure 8, the variation of the coefficients with the wavelength can be important particularly in the regions where the spectral-response matching is not very good [cf. Figure 7(a)]. When the system is perfect, such coefficients are independent of the wavelength. For the not-very-well-matched system used herein, the fluctuations are important particularly near the feet of the *XYZ* peaks. The contributions of filter i to the *XYZ* component can be written as follows:

$$X^i = \Sigma_\lambda S_\lambda R^i_\lambda [C^i_{\text{ref}} + \delta C^i_\lambda]$$

where S_λ is the stimulus that these authors want to measure and R_λ is the spectral response of the system. The calibration coefficient C is written with a fixed contribution and a correction dependent on the wavelength. The quantity measured with filter i is given by

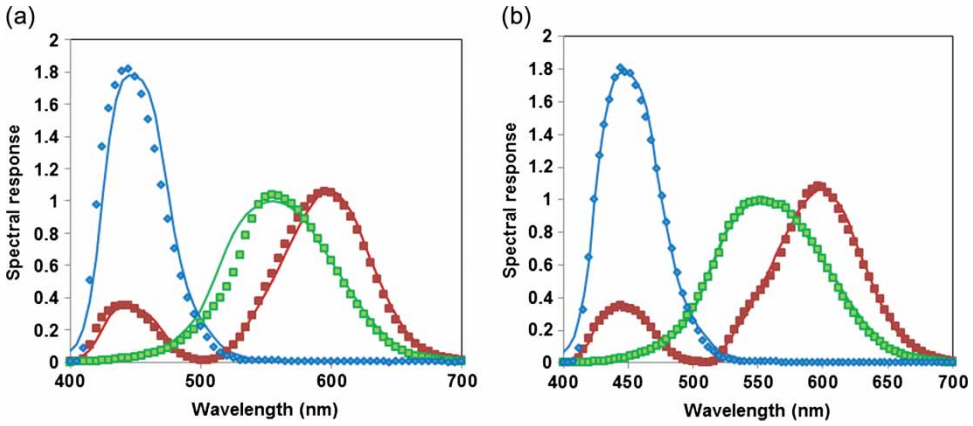

Figure 7. CIE matching for two videocolorimeters, one with (a) limited spectral matching and one with (b) excellent color matching.

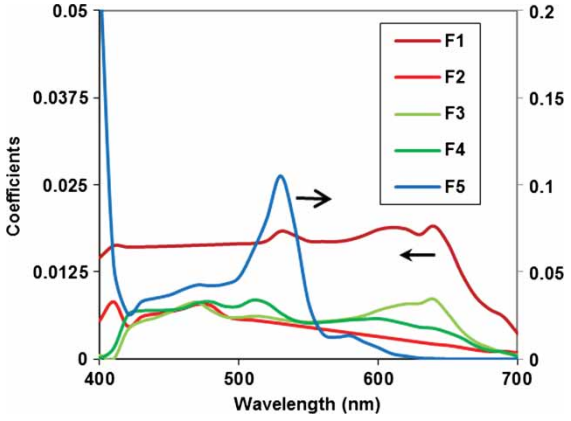

Figure 8. Optimized coefficient for the five color filters shown in Fig. 6 and 7(a)

$$M^i = \Sigma_\lambda S_\lambda R^i_\lambda \tag{12}$$

The best calibration coefficient C^i to measure stimulus S_λ will be obtained if

$$M^i C^i = X^i.$$

Thus, the best coefficient is given by

$$C^i = C^i_{\text{ref}} + \frac{\Sigma_\lambda S_\lambda R^i_\lambda \delta C^i_\lambda}{(\Sigma_\lambda S_\lambda R^i_\lambda)}. \tag{13}$$

In other words, the deviations of the calibration coefficients must be weighted by a coefficient depending on the spectrum itself and the spectral response at each wavelength. If the spectrum is known *a priori*, the coefficient can be calculated by allowing exact color measurements for this stimulus. Of course, under realistic conditions, the spectrum is not perfectly known, but the stability of the method is ensured by the fact that the spectral dependence induces only a correction with regard to the standard calibration based on fixed calibration coefficients.

One example of an application using a CCFL lamp and different color filters is shown in Table 1. The light source is a CCFL backlight that has been stabilized and homogenized for calibration purposes [15]. Eleven color filters are added on top of the CCFL lamp to the obtained colors that cover a large part of the chromatic plane. The system with the spectral response shown in Figure 7(a) is used. Standard calibration adjusting the five coefficients of the color filters, as shown in Figure 7(a), produces colors with quite large errors both for the luminance and the color (see the first set of color and luminance errors in Table 1). Assuming that the emission spectra of the different color stimuli are known *a priori*, a new set of coefficients can be computed using the spectral dependence of the coefficients shown in Figure 8 and Equation (13). Of course, the real spectra can differ from the theoretical spectra used for the computation. To illustrate this point, spectra with different spectral resolutions were introduced. As the CCFL emission spectra present a series of sharp peaks, this modification induces substantial differences in the results. Luminance and color errors obtained with two sets of coefficients calculated with 6 and 12 nm spectral resolutions are also presented in Table 1 (the second and third sets of color and luminance errors). The reduction of the errors compared to those obtained using the standard coefficients is spectacular even for the lower spectral resolution. This response stability is a consequence of the spectral-response matching with the CIE curves even if in this case, it is not very good [cf. Figure 7(a)].

4.2. *Color locus correction*

If the spectrum is not known, the color coordinates obtained with the standard set of coefficients can be used as the starting values, and weighting a new set of coefficients depending on the distance of these color coordinates points to different monochromatic calibrated wavelengths (cf. Figure 9). More precisely, if (u_0, v_0) refers to the measured color coordinates of one pixel of the image using the standard calibration coefficients, and if (u_λ, v_λ) refers to the color coordinates of each calibrated point on the spectral locus, distance d_λ between the two color points can be

Table 1. Color accuracy obtained on a CCFL lamp with color filters with standard calibration and spectral correction, using the different spectral resolutions.

	White	Red	Orange	yellow	green1	green2	green3	green4	Cyan	Blue	Magenta
Measurement with SR3											
X	224.92	72.96	275.03	327.28	162.63	10.50	48.24	7.13	50.28	26.22	167.39
Y	211.55	34.21	161.03	312.58	233.23	30.04	18.84	19.86	66.96	13.04	77.11
Z	163.60	0.35	53.64	14.07	43.44	1.42	87.86	21.35	189.67	140.99	118.17
x	0.375	0.679	0.562	0.500	0.370	0.250	0.311	0.148	0.164	0.145	0.462
y	0.353	0.318	0.329	0.478	0.531	0.716	0.122	0.411	0.218	0.072	0.213
Standard calibration											
X	225.72	71.38	274.51	331.02	166.70	11.13	46.82	7.13	49.09	24.61	163.49
Y	211.13	32.03	157.83	315.77	235.34	30.65	17.36	18.57	64.63	11.29	72.22
Z	159.48	0.57	53.81	12.38	37.28	1.01	88.64	18.47	183.16	138.03	118.41
x	0.379	0.687	0.565	0.502	0.379	0.260	0.306	0.161	0.165	0.141	0.462
y	0.354	0.308	0.325	0.479	0.536	0.716	0.114	0.420	0.218	0.065	0.204
Color error	0.0040	0.0129	0.0052	0.0020	0.0104	0.0098	0.0094	0.0168	0.0016	0.0085	0.0087
Y error	-0.20%	-6.39%	-1.99%	1.02%	0.91%	2.03%	-7.84%	-6.50%	-3.47%	-13.47%	-6.34%
Spectral correction with spectral resolution 6nm											
X	224.78	72.90	274.86	327.15	162.62	10.51	48.17	7.14	50.21	26.15	167.20
Y	212.31	34.13	160.86	313.61	234.45	30.26	18.79	20.00	67.42	13.07	76.95
Z	163.50	0.34	53.55	14.13	43.54	1.43	87.73	21.36	189.51	140.79	117.99
x	0.374	0.679	0.562	0.500	0.369	0.249	0.311	0.147	0.163	0.145	0.462
y	0.354	0.318	0.329	0.479	0.532	0.717	0.121	0.412	0.220	0.073	0.212
Color error	0.0011	0.0005	0.0002	0.0013	0.0016	0.0019	0.0001	0.0015	0.0014	0.0003	0.0002
Y error	0.36%	-0.23%	-0.11%	0.33%	0.53%	0.73%	-0.23%	0.68%	0.69%	0.22%	-0.21%
Spectral correction with spectral resolution 12nm											
X	224.49	72.77	274.51	326.81	162.53	10.50	48.05	7.14	50.10	26.04	166.84
Y	213.68	33.98	160.52	315.41	236.65	30.66	18.72	20.24	68.28	13.13	76.64
Z	163.45	0.34	53.47	14.28	43.70	1.44	87.57	21.38	189.35	140.54	117.79
x	0.373	0.680	0.562	0.498	0.367	0.246	0.311	0.146	0.163	0.145	0.462
y	0.355	0.317	0.329	0.480	0.534	0.720	0.121	0.415	0.222	0.073	0.212
Color error	0.0031	0.0014	0.0004	0.0036	0.0047	0.0055	0.0003	0.0044	0.0039	0.0009	0.0005
Y error	1.01%	-0.69%	-0.32%	0.90%	1.47%	2.07%	-0.62%	1.92%	1.98%	0.68%	-0.61%

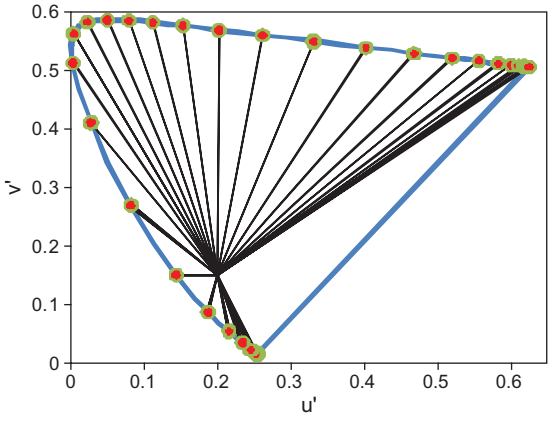

Figure 9. Principle of color locus correction.

calculated using the following equation:

$$d_\lambda = \sqrt{(u_0 - u_\lambda)^2 + (v_0 - v_\lambda)^2},$$

and $1/d_\lambda$ can be used as the weighting coefficient to obtain the new calibration coefficient in the same way as previously, using the following equation:

$$C^i = C^i_{\text{ref}} + \frac{\Sigma_\lambda \frac{R^i_\lambda \delta C^i_\lambda}{d_\lambda}}{\Sigma_\lambda \frac{R^i_\lambda}{d_\lambda}}. \tag{14}$$

One example of the application of this method is reported for the system with the spectral response shown in Figure 7(a), and using various double Gaussian spectral stimuli. More precisely, different spectral stimuli are generated by changing the wavelength position and the width of the two Gaussian peaks to cover a large part of the chromatic plane. For each spectrum, the color obtained with the standard calibration coefficients is first computed, and a new set of coefficients is computed using Equation (14). The color error is evaluated for the two sets of coefficients, and the results are shown in Figure 10(a) and (b). The color error is more or less decreased depending on its location on the $u'v'$ plane and on the spectrum of the stimulus. In practice, there is no degradation of color accuracy anywhere in the chromatic plane. The main advantage is that the user does not need any *a priori* knowledge of the spectrum, but post-measurement computing is needed for each pixel of the image. This method works well for near-monochromatic stimuli like color LEDs.

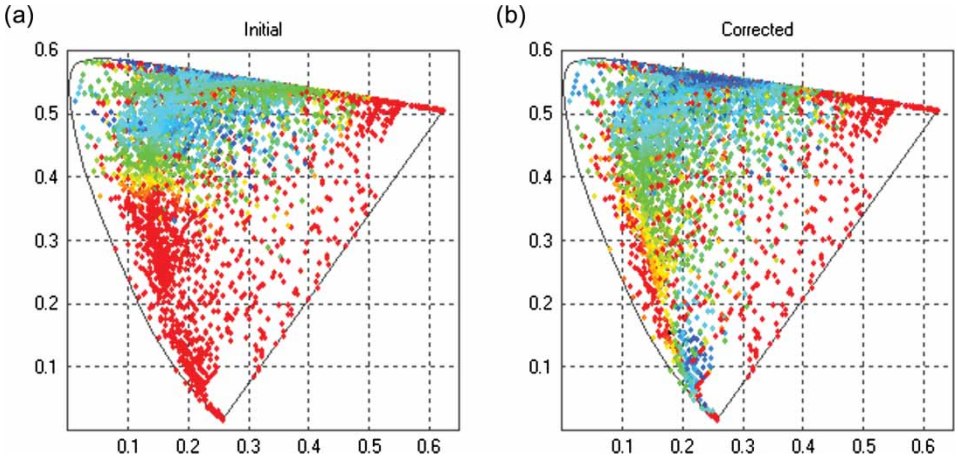

Figure 10. (a) Color measurement error for double Gaussian stimuli with standard coefficients. (b) Color locus correction. The maximum scale error in red is fixed at 0.02.

4.3. Tristimulus calibration

Tristimulus calibration seems very attractive for display measurements because the light emission is basically a combination of the three different spectra emitted by the R, G, and B pixels. In theory, any tristimulus colorimeter, even with a spectral response that does not match the CIE curves, can make color measurements under such conditions without any colorimetric error. Indeed, the RGB values measured on the three colors' pixels can be made to correspond exactly with the XYZ values of the colors using a 3×3 matrix. This explains why many people think that the performance of tristimulus calibration can enable accurate color measurements on displays using any type of tristimulus colorimeter and even with color CCD sensors with Bayer filter mosaic. This is claimed even by some manufacturers of measurement instruments. Unfortunately for the customer, this is true only when the measured source is an exact linear combination of the primary colors used for the calibration. In practice, however, this is never the case because of the fluctuations of the spectral characteristics between the different panels or versus the angle, temperature, or many other parameters. The black state is also critical in this respect because it is never a linear combination of the three primary colors. The interest in a filter colorimeter with good CIE matching stems from the stability of the tristumulus calibration with regard to unavoidable fluctuations.

To illustrate this point, the color error on an RGB LED source when the mean wavelength positions of the primary colors are slightly changing is computed. This example is important because most of the existing LCD panels include LEDs for backlighting and OLED panels exhibit this type of spectra. The typical spectral characteristics of this source are shown in Figure 11. In the following, the use of two types of tristimulus colorimeters – a color CCD camera with integrated Bayer filters that do not match the CIE curves and an imaging system with five filters quite correctly matching the CIE curves [cf. Figure 7(a)] – is simulated. The tristimulus calibration is carried out using the two systems on the three

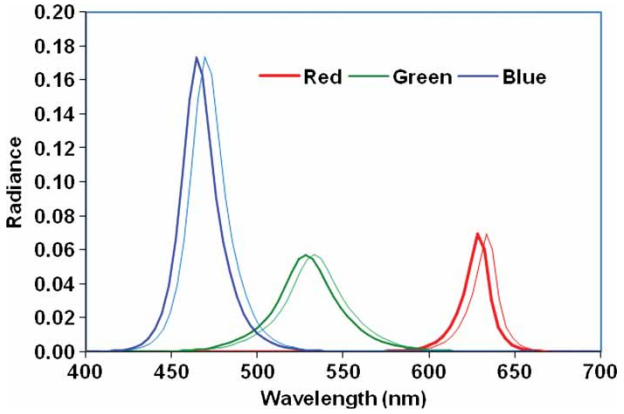

Figure 11. Typical spectra of red, green, and blue LEDs. The spectra with 5-nm shifts are also shown.

reference RGB LED spectra shown in Figure 11. In the case of the color CCD sensor, it is used for straightforward calculation. For the five-filter system, the matrix is optimized to minimize the correction terms [15,16]. Then a minimal (2 or 5 nm) spectral shift of the three primaries is assumed. This shift is similar to what can be observed during the thermal cycle of one LED or from one LED to another in the same fabrication batch (cf. Figure 11). The colorimetric errors obtained with the two instruments while measuring the variable linear combinations of such spectra are shown in Figure 12 for the color CCD camera and for the five-filter system. The much higher stability of the CIE-matched instrument is evident.

5. Conclusion

In this paper, it is shown that CIE spectral-response matching is mandatory to achieve color accuracy using imaging-filter-based colorimeters. If the spectral response of the system is well matched to the CIE curves, the color accuracy will be good for any kind of light source. In addition,

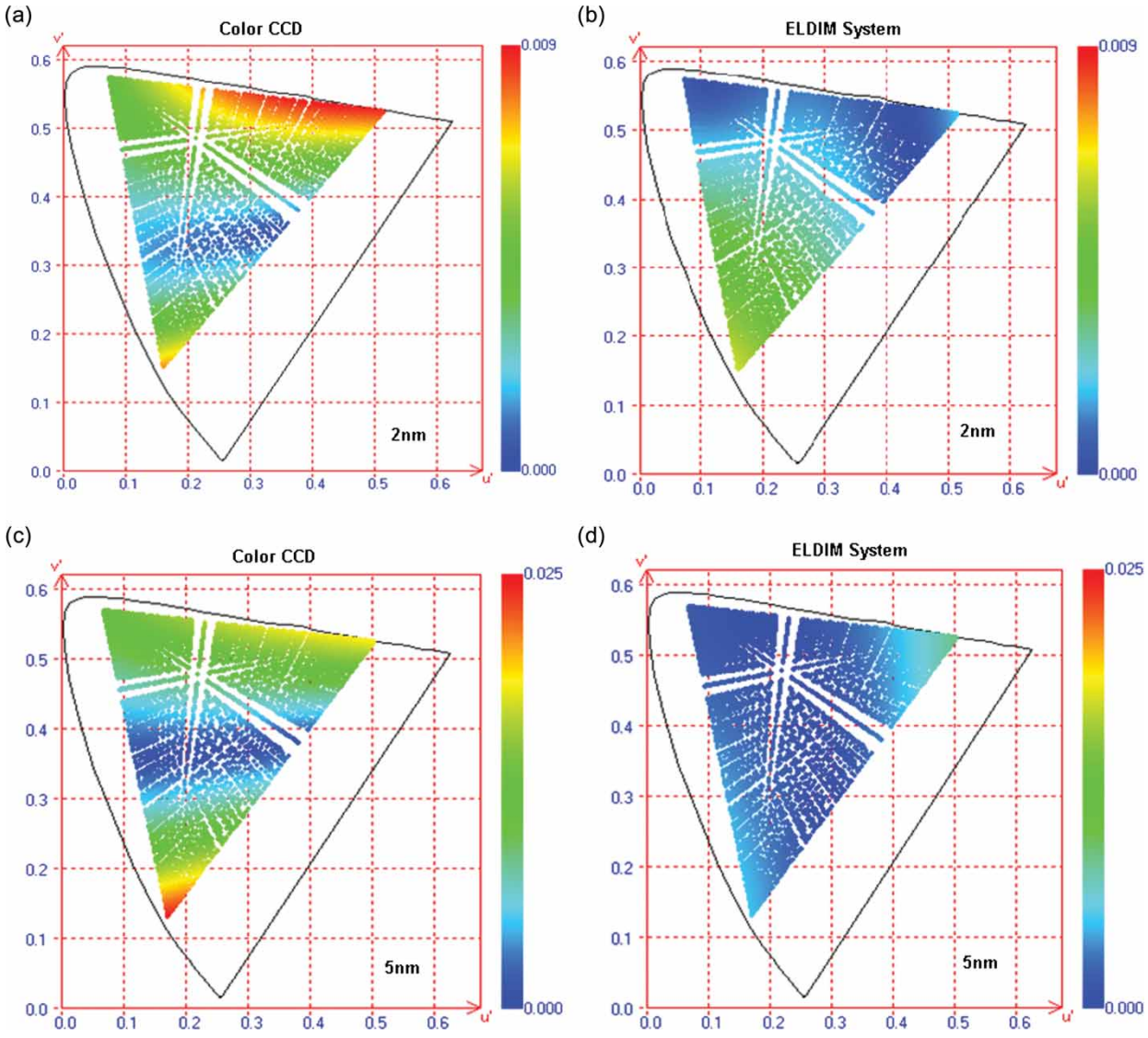

Figure 12. Colorimetric error in $u'v'$ after tristimuli calibration for the color CCD sensor [(a) and (c)] and the five-color-filter system [(b) and (d)] for a wavelength shift on the RGB LED emissions of 2 nm [(a) and (b)] and 5 nm [(c) and (d)].

different methods of increasing the color accuracy are proposed, using the real spectral response of the system. If there is partial knowledge of the spectral properties of the target, better color accuracy can be obtained using the corrected coefficients. In addition, even if no information is available for the target, some corrections can be made using the color locus correction method. Tristimulus calibration is applicable for many practical situations where the color is reproduced with three primaries (e.g. printing, displays). Nevertheless, this method works well only if it corrects the basic measurements. Otherwise, its application domain will be extremely reduced, and a small spectral variation on the target can lead to very high color errors. This is why much effort is made by these authors to match the response of the proposed instruments to the CIE curves.

References

[1] W. Wu, J. Allebach, and M. Analoui, *J. Imaging Sci. Technol*. **44**, 4, 267 (2000).

[2] S. Henker, J. Schlussler, and R. Schuffny, *Proceedings of the VIIth Digital Image Computing*, Vol. 771, 10–12 December, Sydney, Australia, 2003.

[3] N. Ohta, *Col. Res*. **7**, No. 1, 76 (2001).

[4] T. arEjaz, Y. Shoichi, T. Horiuchi, T. Yokota, M. Takaya, G. Ohashi, and Y. Shimodaira, *Proc. SPIE* **5667**, 146 (2005).

[5] M. Kuramoto, Y. Iwaki, H. Urabe, and H. Sugiura, *Annual Meeting Summary of SPSTJ*, Tokyo, Japan, Vol. 68, no. 1, 2005, p. 26.

[6] I. Ghiczy, J. Hawthorne, K. Muray, I. Rety, and J. Schanda, *13th International Display Research Conference*, Strasbourg, France, August 31–September 3, 1993.

[7] K. Muray and J. Schanda, *CORM Meeting*, Ottawa, Canada 1995.

[8] T. Ejaz, T. Horiuchi, G. Ohashi, and Y. Shimodaira, *IEICE Trans. Electron*. **E89-**C, No. 10, 1441–1447 (2006).

[9] R. Luther, *Z. Technol. Phys*. **8**, 540 (1927).

[10] Y. Ohno and J. Hardis, *Proceedings of the IS&T/SID Fifth Color Imaging Conference*, Scottsdale, Arizona, USA, 1997, pp. 301–305.

[11] Y. Ohno Y. and S.W. Brown, *Proceedings of the IS&T/SID Sixth Color Imaging Conference*, Scottsdale, Arizona, USA, 1998, pp. 65–68.

[12] Wyszecki Gunter, *Color Science*, 2nd ed., Wiley-Interscience Publication, John Wiley & Sons, New York, 2000, pp. 725–733.

[13] S. Pattanaik and K. Torrance, Technical Report PCG-98-1 Cornell University Program of Computer Graphics, Ithaca, NY, 1998

[14] T. Larason, S. Bruce, and C. Cromer, *J. Res. Natl. Inst. Technol*. **101**, 133, (1996).

[15] T. Leroux, T. Bignon, E. Chauvat, and P. Boher, *SID Meeting*, San Francisco, USA, June 4–9, 2006, p. 74.

[16] Z. Kosztyan, G. Eppeldauer, and J. Schanda, *Appl. Optics* **49**, 12, 2288–2301 (2010).